journal

J. Am. Ceram. Soc., 94 [12] 4352–4357 (2011)
DOI: 10.1111/j.1551-2916.2011.04712.x

Normal to Relaxor Ferroelectric Transition and Domain Morphology Evolution in (K,Na)(Nb,Sb)O_3–$LiTaO_3$–$BaZrO_3$ Lead-Free Ceramics

Ruzhong Zuo,[‡,†] Jian Fu,[‡] Shengbo Lu,[§] and Zhengkui Xu[§]

[‡]Institute of Electro Ceramics & Devices, School of Materials Science and Engineering, Hefei University of Technology, Hefei, 230009, China

[§]Department of Physics and Materials Science, City University of Hong Kong, Hong Kong, China

A normal to relaxor ferroelectric transition was induced by the substitution of $BaZrO_3$ for $LiTaO_3$ in a typical lead-free (K,Na)(Nb,Sb)O_3–$LiTaO_3$–$BaZrO_3$ system and this was found to accompany a tetragonal to rhombohedral phase structural transformation. The typical relaxor behavior characterized by diffuse phase transition and frequency dispersion was identified by the measurement of frequency-dependent dielectric permittivity. The transmission electron microscopy studies demonstrated that the above phenomenon would be closely related to the domain morphology evolution from normal micron-sized lamellar domains, to tweed-like domains and finally to polar nanodomains. Selected area and convergent beam electron diffraction patterns further confirmed that the composition (2.5 mol% $BaZrO_3$) exhibited rhombohedral and tetragonal phase coexistence. The evolution of domain morphology with temperature also disclosed the diffuseness of ferroelectric phase transition.

I. Introduction

THE $(Na_{0.5}K_{0.5})NbO_3$ (NKN) based lead-free piezoelectric ceramics have been widely investigated in the past few years, particularly for Li, Ta, and Sb-modified NKN compositions.[1–7] These lead-free ceramics have exhibited advantages such as relatively high Curie temperatures (T_c) and good piezoelectric properties over other lead-free piezoelectric ceramic systems, for example, $BaTiO_3$ (BT)- or $(Bi_{0.5}Na_{0.5})TiO_3$ (BNT)-based compositions.[8–10] Enhanced piezoelectric performances of these compositions were generally considered to originate from the coexistence of the orthorhombic and tetragonal ferroelectric phases[11–14] or the rhombohedral and orthorhombic ferroelectric phases.[15,16] The formation of the two-phase coexistence zone was achieved simply by shifting the polymorphic phase transitions in NKN close to room temperature. We recently reported modified NKN compositions with coexisting rhombohedral and tetragonal ferroelectric phases at room temperature,[17] which is similar to the traditional phase boundary in conventional lead-based piezoelectric ceramics such as $Pb(Zr,Ti)O_3$.[18] It was found that the substitution of $BaZrO_3$ for $LiTaO_3$ tends to shrink the orthorhombic phase zone by increasing the temperature range of the rhombohedral phase at low temperature side.[17]

Furthermore, the dielectric permittivity variation against temperature for the above composition was found to be more and more diffuse with an increase in the substitution. The pure NKN ceramic was generally considered to be a normal ferroelectric as can be judged from its dielectric behavior.[19] However, the diffuse phase transition behavior or relaxation behavior was often induced as some dopants were introduced into NKN lattices.[20–24] In lead-based piezoelectric compositions,[25] it has been found that the normal to relaxor ferroelectric phase transition usually corresponded to the structural phase transformation from tetragonal to rhombohedral phase. It was also suggested that the above structural phase transformation and normal-relaxor ferroelectric transition would accompany the domain morphology evolution.[26,27] To a better understanding of the dielectric and ferroelectric behavior of NKN-based ceramics from the viewpoint of domain configurations, it is necessary to investigate the ferroelectric domains for which a lot of work in the past was focused on lead-based piezoelectric systems[28–30] and some lead-free piezoelectric such as BT- and BNT-based compositions.[31–35] To the knowledge of the authors, so far little work has been done on the domain morphology evolution in NKN-based lead-free ceramics. Particularly, the correlation between the domain configuration, the phase structural transformation, and electrical properties was not yet studied in these compositions.

The objective of this work is thus to explore the effect of the substitution of $BaZrO_3$ for $LiTaO_3$ on the domain morphology evolution in $(Na_{0.52}K_{0.40})(Nb_{0.84}Sb_{0.08})O_3$–$(0.08-x)LiTaO_3$–$xBaZrO_3$ (NKNS–LT–xBZ) lead-free piezoelectric ceramics by means of transmission electron microscopy, and to give an in-depth understanding of the transition from normal to relaxor ferroelectric at the microscopic domain level. Special attention was paid to the rhombohedral and tetragonal phase boundary composition where the coexistence of normal and relaxor ferroelectric phases was demonstrated.

II. Experimental Procedure

The NKNS–LT–xBZ ceramics (x = 0, 0.025, and 0.05) were prepared by a solid-state reaction method. The detailed experimental procedure was reported previously.[17] The room-temperature crystal structures of all three sintered specimens were examined by an X-ray diffractometer (XRD, D/MAX2500VL/PC; Rigaku, Tokyo, Japan). The dielectric permittivity of unpoled samples sintered at optimal temperatures was measured as function of temperature (25°C–350°C) and frequency (0.1–1000 kHz) by means of an LCR meter (E4980A; Agilent, Santa Clara, CA). After silver paste was fired on major surfaces at 550°C for 30 min, polarization vs electric field (P–E) hysteresis loops were measured using a ferroelectric-measuring system (Precision LC, Radiant Technologies Inc., Albuquerque, NM). The domain morphology

D. W. Johnson—contributing editor

Manuscript No. 29541. Received March 31, 2011; approved May 21, 2011.

This work was financially supported by National Natural Science Foundation of China (50972035) and a Program for New Century Excellent Talents in University, State Education Ministry (NCET-08-0766) and also partially supported by a grant from the Research Grants Council of the Hong Kong Special Administrative Region, China (No. 9041211).

[†]Author to whom correspondence should be addressed. e-mail: piezolab@hfut.edu.cn

observation and selected area electron diffraction (SAED) were performed on a transmission electron microscope (TEM, Phillips CM-20, Hillsboro, OR) operated at 200 kV with a charge-coupled device camera. In addition, convergent beam electron diffraction (CBED) patterns were recorded at 120 kV. For TEM examination, samples were first mechanically polished to a thickness of ~20 μm and then ion-milled on a Gatan Dual Ion Mill unit (Model 600) at 5 kV. All specimens were annealed at 80°C for at least one day to release the stress.

III. Results and Discussion

The dielectric permittivity of NKNS–LT–xBZ ceramics with changing temperature and frequency is shown in Fig. 1(a). It can be seen that a relatively sharp dielectric peak corresponding to the ferroelectric-paraelectric phase transition appears at ~250°C for the sample with $x = 0.01$. Moreover, a weak frequency dependence of the temperature (T_m) corresponding to the dielectric maximum (ε_m) can be seen. However, with increasing BZ concentration, the dielectric peaks become more and more diffuse. In particular, the frequency dispersion becomes more distinct, because ε_m obviously decreases and T_m shifts toward higher temperatures with increasing frequency. The XRD patterns of all three specimens [Fig. 1(b)] indicate typical perovskite structures with different crystal symmetry. The transition from rhombohedral to tetragonal phases can be identified with decreasing BZ content x. The composition with $x = 0.025$ may have a coexistence of rhombohedral and tetragonal phases, as manifested by split (200) diffraction peaks [inset in Fig. 1(b)]. The detailed analysis about phase transformation was reported previously.[17]

The relaxor ferroelectrics are known to have the diffuse phase transition (DPT) and the frequency dispersion of the dielectric permittivity. For a normal ferroelectric, the dielectric permittivity above T_c obeys the Curie–Weiss law,

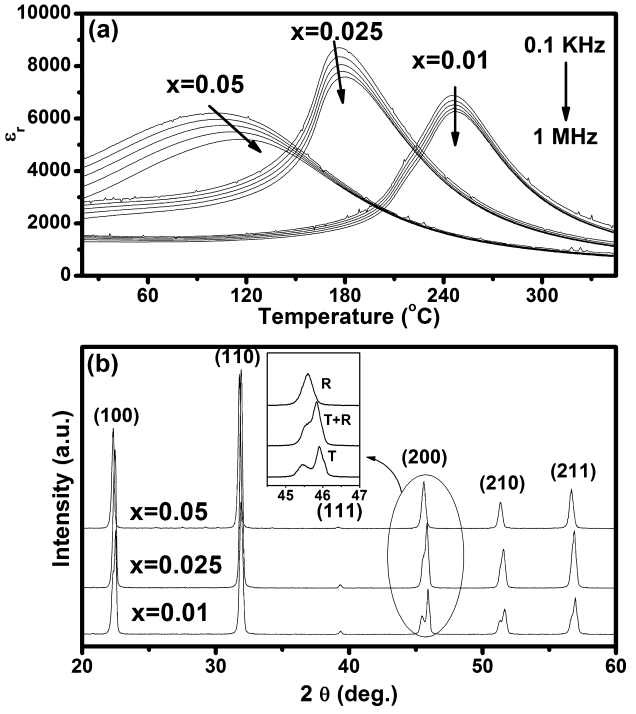

Fig. 1. (a) Curves of dielectric permittivity vs temperature and frequency for NKNS–LT–xBZ samples as indicated, and (b) the corresponding X-ray diffraction patterns (insets are the magnified (200) diffraction peaks).

$$\frac{1}{\varepsilon} = \frac{T - T_c}{C_1} (T > T_c) \quad (1)$$

where C_1 is the Curie–Weiss constant. The inverse dielectric permittivity measured at 100 kHz was plotted as a function of temperature, as shown in Fig. 2. It is found that the dielectric permittivity of NKNS–LT–xBZ ceramics more obviously deviates from the Curie–Weiss law with increasing BZ content. The deviation degree from the Curie–Weiss law can be defined by ΔT_m as follows:

$$\Delta T_m = T_{cw} - T_m \quad (2)$$

where T_{cw} denotes the temperature from which the dielectric permittivity starts to deviate from the Curie–Weiss law. When $T < T_{cw}$, the paraelectric phase transforms into the ergodic relaxor state and thus forms the polar nanoregions (PNRs).[36] It is found that the calculated ΔT_m increases from 34°C to 106°C, and finally to 127°C with an increase in the BZ content x from 0.01 to 0.05, indicating that the DPT behavior was enhanced gradually with increasing BZ content. For a ferroelectric with DPT, the diffuseness of the paraelectric–ferroelectric phase transition can be more effectively described by a modified Curie–Weiss law,[37]

$$\frac{1}{\varepsilon} - \frac{1}{\varepsilon_m} = \frac{(T - T_m)^\gamma}{C_2}, 1 \le \gamma \le 2 \quad (3)$$

where C_2 is the Curie constant, and γ is the indicator of the diffuseness degree, ranging between 1 for a normal ferroelectric and 2 for a complete DPT ferroelectric. The plots of log $(1/\varepsilon - 1/\varepsilon_m)$ as a function of log $(T - T_m)$ at 100 kHz are also shown in Fig. 2 (see insets). The γ value can be determined from the slope of the fitted lines. It can be seen that the γ value increases from 1.51 to 1.92 with an increase in the BZ content. Large values of γ and ΔT_m reveal that all studied compositions exhibit obvious DPT behavior. Particularly, the NKNS–LT–0.05BZ sample shows nearly complete DPT. However, this feature cannot confirm whether NKNS–LT–xBZ samples are the relaxor ferroelectrics because many nonrelaxor ferroelectrics also have DPT.[38]

The parameter ΔT_{relax} was often introduced to investigate the relaxation degree of ferroelectric ceramics,[39] which is defined as the difference between two T_m values measured at 100 kHz and 100 Hz, respectively. Based on the experimental data, the value ΔT_{relax} was calculated to be about 1.5°C for $x = 0.01$, indicating a very weak frequency dispersion. However, the value increases to ~10°C for $x = 0.05$, meaning that the frequency dispersion was significantly increased owing to the substitution of BZ for LT. Moreover, the relaxor ferroelectrics were found to be similar to spin glass systems in magnetism. As a result, the relaxation behavior follows an empirical Vogel–Fulcher relation, which can be also employed to determine the dielectric relaxation feature.[38] According to this relationship, the frequency f was described as follows:

$$f = f_0 \exp[-E_a/k(T_m - T_f)] \quad (4)$$

where f_0 is the Debye frequency, E_a is the activation energy (the barrier between equivalent polarization state), k is the Boltzmann constant, and T_f is the freezing temperature of the dynamics of PNRs. The values of the inverse $(T_m - T_f)$ for NKNS–LT–xBZ ceramics were plotted as a function of lnf and linearly fitted with the Vogel–Fulcher law, as shown in Fig. 2(d). The values of E_a, T_f, and f_0 can be then determined from the slope and intercept of the fitted lines, as listed in Table I. It can be seen that there is only a slight

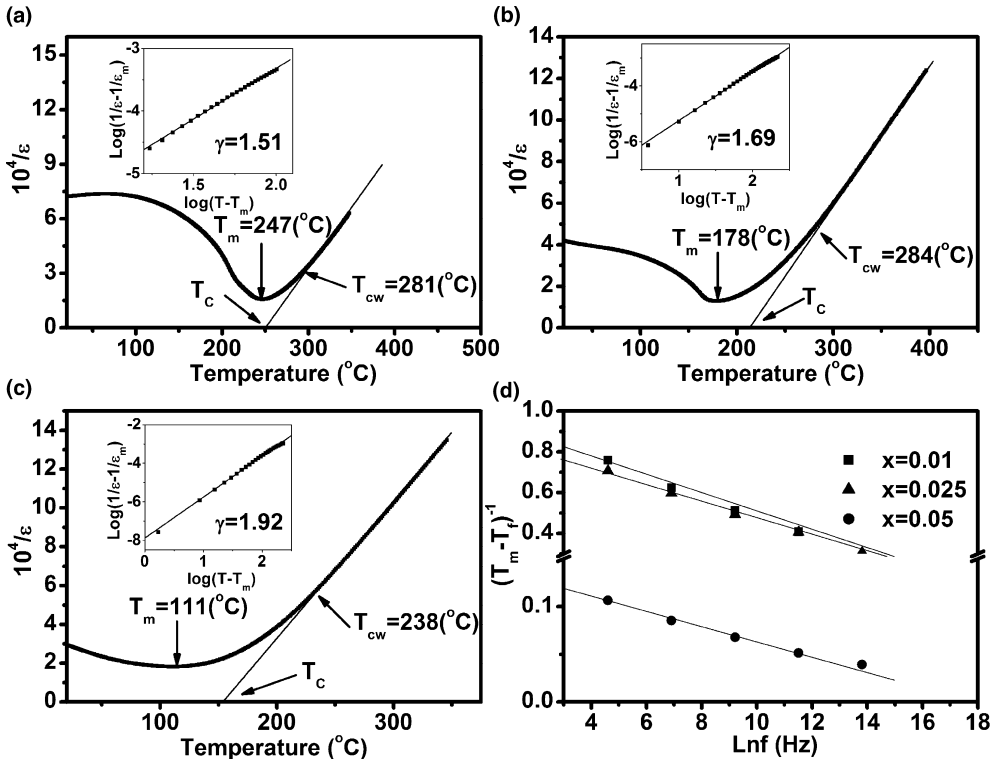

Fig. 2. Inverse dielectric permittivity at 100 kHz as a function of temperature for NKNS–LT–xBZ samples: (a) $x = 0.01$, (b) $x = 0.025$, and (c) $x = 0.05$ (insets are the corresponding curves of $\log(1/\varepsilon - 1/\varepsilon_m)$ against $\log(T - T_m)$ at 100 kHz), and (d) the inverse $(T_m - T_f)$ vs *lnf* curves linearly fitted with the Vogel–Fulcher law.

Table I. The Various Physical Parameters Calculated from Vogel–Fulcher Analysis for NKNS–LT–xBZ Ceramics as Indicated

x	E_a (eV)	T_f (°C)	f_0 (Hz)
0.01	0.021	244.2	2.04×10^9
0.025	0.024	175.4	2.55×10^9
0.05	0.087	91.3	5.22×10^8

increase for E_a as the BZ content changes from $x = 0.01$ to $x = 0.025$, but a rapid increase from $x = 0.025$ to $x = 0.05$. Moreover, it is also noted that T_f is near T_m for $x = 0.01$ and 0.025, but far below T_m for $x = 0.05$. Both changes of E_a and T_f mean that NKNS–LZ–xBZ composition with high BZ content is a typical relaxor ferroelectric.[36] These results reveal that the NKNS–LZ–xBZ ceramics show a "relaxor-like" characteristic at low BZ concentration ($x = 0.01$) but a typical relaxor behavior at high BZ concentration ($x = 0.05$), indicating that the composition with $x = 0.025$ should lie close to the transitional zone between normal and relaxor ferroelectric states. Similar phenomenon was found in (Pb, La)$(Zr,Ti)O_3$ with a critical La content where the relaxor and normal ferroelectric behaviors coexist.[40]

From the above results, it is clear that the addition of BZ has induced a spontaneous normal tetragonal to relaxor rhombohedral ferroelectric phase transformation. This kind of phase transition behavior may be accompanied by the corresponding change of domain switching behavior and domain morphology. Electric field-induced polarization hysteresis loops were measured at 1 Hz for all three NKNS–LT–xBZ samples, as shown Fig. 3. A saturated square hysteresis loop was observed for the sample with low BZ concentration, showing a relatively large spontaneous polarization (P_s) and remnant polarization (P_r). This is a typical characteristic of the phase that contains long-range interaction between dipoles and owns micron-sized ferroelectric

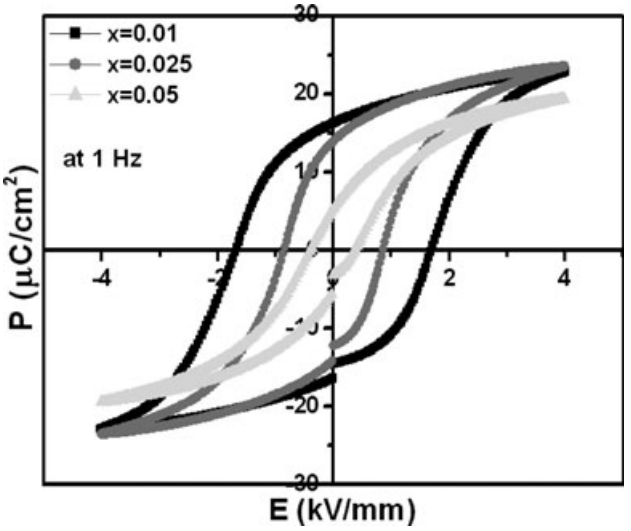

Fig. 3. Polarization vs electric field hysteresis loops of NKNS–LT–xBZ samples as indicated.

domain state,[41] indicating that NKNS–LT–xBZ ceramics with low BZ content belongs to a normal ferroelectric. With an increase in the BZ content, the loops become much slimmer, particularly for the $x = 0.05$ sample with a rhombohedral relaxor ferroelectric state. Compared to the P_r value, the saturated polarization (P_{max}) for the sample with $x = 0.05$ is only slightly less than the value for samples with $x = 0.01$ and $x = 0.025$. The results indicate that the polarization of rhombohedral phase can be aligned to the saturated state but cannot be maintained when the applied electric field is removed. The relaxor behavior of ferroelectrics was generally considered to originate from the local order–disorder of the crystal structure which causes the formation of PNRs and

local electric field, owing to the heterovalent occupation of A-site and B-site by Ba^{2+} and Zr^{4+}, respectively. The presence of the random field can hinder the long-range dipole alignment and thus suppress the ferroelectric interaction, resulting in a lower P_s value. Although the normal ferroelectric state with long-range dipoles in a relaxor ferroelectric can be excited by electric field (i.e., larger P_{max}),[42] yet it cannot be maintained after the external electric field is released. As a result, the sample finally exhibits a lower P_r. In addition, it is also believed that the absence of long-range dipoles restricts not only the polarization but also tends to induce the formation of polar nanodomains.[43]

The domain morphology of NKNS–LT–xBZ ceramics was observed by TEM, as shown in Fig. 4. It can be seen that normal micron-sized lamellar domain structures are dominant in the sample with $x = 0.01$ [Fig. 4(a)]. However, the domain morphology becomes tweed-like for the composition with $x = 0.025$, illustrating the coexistence of the normal ferroelectric phase with minor relaxor phase.[40] With further increase in the BZ content, the micron-sized domains disappeared and only polar nanodomains can be found [Fig. 4(c)], which are typical of relaxor ferroelectrics.[27,44,45] Therefore, the transition from normal tetragonal to rhombohedral relaxor ferroelectric phases was found to correlate with the domain morphology evolution from normal micro-sized domains, to tweed-like domains and finally to polar nanodomains. The results keep good agreement with the feature of the dielectric response (Figs. 1 and 2).

The observation of domain morphology simply indicates that the $x = 0.025$ composition may be at the critical point from tetragonal to rhombohedral phase transitions. This conclusion can be strongly supported by further TEM studies. As shown in Fig. 5(a), the SAED pattern was taken along the <001> zone axes in which the <1/2, 1/2, 0> superlattice was observed, indicating the presence of the rotation of the oxygen octahedra according to the $a^0a^0c^+$ in-phase octahedral tilting. The phenomenon is similar to that in $(Bi_{0.5}Na_{0.5})TiO_3$ where the $a^0a^0c^+$ was related to the high-temperature tetragonal phase.[33] Therefore, it was suggested that the tetragonal phase should exist in NKNS–LT–0.025BZ sample. However, <1/2, 1/2, 0> superlattice was found in SAED patterns along the <001> zone axes but not along the <110> zone axes in the in-phase octahedron-tilt system.[34] As a result, no <110> zone axes-forbidden reflection can be seen, as shown in Fig. 5(b). The CBED was thought of as a popular technique for determining the point group of a crystal because it is possible to obtain the symmetry information from very small regions in a specimen (two CBED patterns were obtained within a single domain in present study).[46] It can be seen from Fig. 5(c) that the fourfold rotation axis was parallel to the [001] and the two mirror planes were parallel to the [100] and [110] between which the angle is 45°. This symmetry pattern is typical of the tetragonal structure with 4mm point group. However, only one threefold rotation axes parallel to the [001] and one mirror plane parallel to the [110] can be observed in Fig. 5(d). It can be believed that the projection of [111] cation displacements in rhombohedral phase onto the cubic (111) plane would lead to a single mirror plane parallel to the [110] axis as viewed along the [001] axis.[47] Therefore, the pattern in Fig. 5(d) usually corresponds to a typical rhombohedral ferroelectric phase with 3 m point group. These results also demonstrate that the rhombohedral and tetragonal phase coexistence occurs in the sample with $x = 0.025$.

The domain morphology of the NKNS–LT–0.025BZ sample changing with temperature was investigated by hot-stage TEM, as shown in Fig. 6. The images were first taken upon heating and then cooling from approximately the same

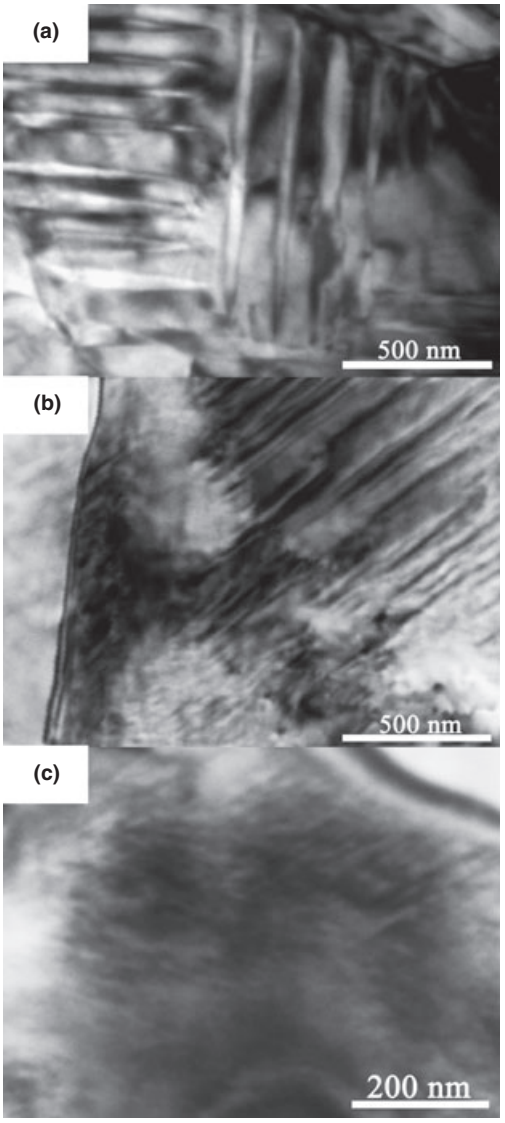

Fig. 4. Bright-field images of NKNS–LT–xBZ samples: (a) $x = 0.01$, (b) $x = 0.025$, and (c) $x = 0.05$.

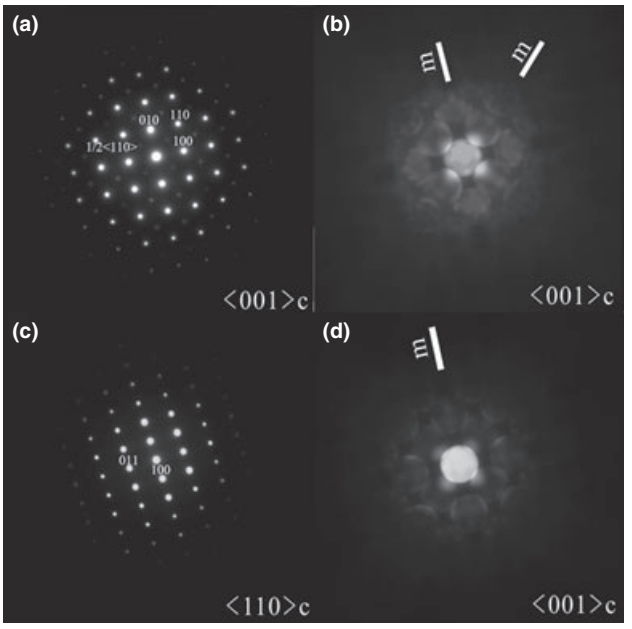

Fig. 5. Selected area electron diffraction patterns for NKNS–LT–0.025BZ samples taken along: (a) < 001 > and (b) < 110 > zone axes and (c, d) convergent beam electron diffraction patterns taken along < 001 > zone axes.

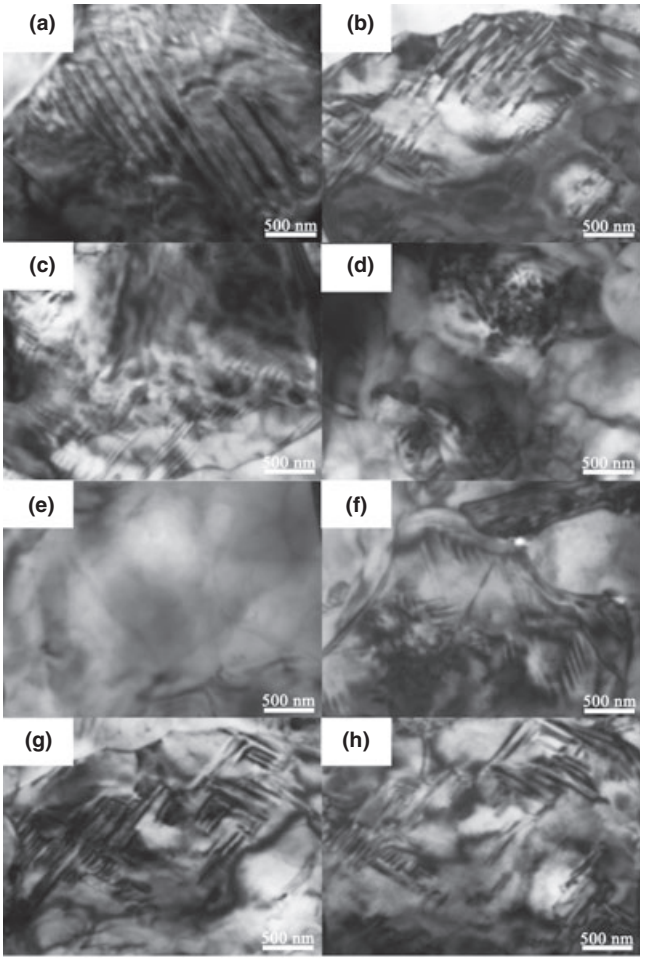

Fig. 6. Temperature-dependent domain structures for NKNS–LT–0.025BZ observed during heating and subsequent cooling: (a) 25°C, (b) 50°C, (c) 175°C, (d) 180°C, (e) 220°C, (f) 180°C, (g) 50°C, and (h) 25°C.

region in the sample. Room-temperature bright-field image [Fig. 6(a)] shows dominant tweed-like domain structures owing to the coexistence of normal and relaxor ferroelectric states. It can be seen that the domain morphology gradually changes with temperature. On the one hand, during heating it starts to become a lamellar domain because the phase structure first changes from the phase coexistence to a single tetragonal phase [Fig. 6(b)].[17] Further heating resulted in a continuous reduction in the domain size, as shown in Fig. 6(c). However, the fine domain striations disappeared and only polar nanodomains were observed when the sample was heated 180°C. This probably results from the existence of PNRs near the ferroelectric phase transition zone. All visible contrast did not completely disappear until 220°C (much higher than the T_m value for this sample), meaning that there exists DPT behavior. On the other hand, it is found that only tweed-like domains were observed during subsequent cooling, as shown in Figs. 6(f)–(h). This phenomenon seems different from that observed in Pb-based relaxor ferroelectrics,[27] where the nanodomains appeared during heating and then could be maintained during subsequent cooling.

IV. Conclusions

The normal to relaxor ferroelectric transition and the corresponding domain morphology evolution for lead-free NKNS–LT–xBZ ceramics were investigated by means of XRD, dielectric measurement, and TEM. The results indicated that the substitution of BZ for LT tends to induce a tetragonal to rhombohedral phase transformation, which was accompanied by a normal to relaxor ferroelectric transition. TEM observation confirmed that the normal to relaxor ferroelectric transition was attributed to the domain morphology evolution from normal micron-sized lamellar domains to polar nanodomains. In addition, the NKNS–LZ–0.025BZ with a tweed-like domain morphology was found to exhibit rhombohedral and tetragonal phase coexistence.

References

[1]Y. Saito, H. Takao, T. Tani, T. Nonoyama, K. Takatori, T. Homma, T. Nagaya, and M. Nakamura, "Lead-Free Piezoceramics," *Nature*, **432**, 84–7 (2004).

[2]E. Hollenstein, M. Davis, D. Damjanovic, and N. Setter, "Piezoelectric Properties of Li- and Ta-Modified $(K_{0.5}Na_{0.5})NbO_3$ Ceramics," *Appl. Phys. Lett.*, **87**, 182905 (2005).

[3]Z. P. Yang, Y. F. Chang, and L. L. Wei, "Phase Transitional Behavior and Electrical Properties of Lead-Free $(K_{0.44}Na_{0.52}Li_{0.04})(Nb_{0.96-X}Ta_xSb_{0.04})O_3$ Piezoelectric Ceramics," *Appl. Phys. Lett.*, **90**, 042911 (2007).

[4]J. G. Wu, Y. Y. Wang, D. Q. Xiao, J. G. Zhu, and Z. H. Pu, "Effects of Ag Content on the Phase Structure and Piezoelectric Properties of $(K_{0.44-X}Na_{0.52}Li_{0.04}Ag_x)(Nb_{0.91}Ta_{0.05}Sb_{0.04})O_3$ Lead-Free Ceramics," *Appl. Phys. Lett.*, **91**, 132914 (2007).

[5]B. Q. Ming, J. F. Wang, P. Qi, and G. Z. Zang, "Piezoelectric Properties of (Li,Sb,Ta) Modified (Na,K)NbO_3 Lead-Free Ceramics," *J. Appl. Phys.*, **101**, 054103 (2007).

[6]R. Z. Zuo, J. Fu, and D. Y. Lv, "Phase Transformation and Tunable Piezoelectric Properties of Lead-Free $(Na_{0.52}K_{0.48-X}Li_x)(Nb_{1-x-Y}Sb_yTa_x)O3$ System," *J. Am. Ceram. Soc.*, **92**, 283–5 (2009).

[7]D. Q. Xiao, J. G. Wu, L. Wu, J. G. Zhu, P. Yu, D. M. Lin, Y. W. Liao, and Y. Sun, "Investigation on the Composition Design and Properties Study of Perovskite Lead-Free Piezoelectric Ceramics," *J. Mater. Sci.*, **44**, 5408–19 (2009).

[8]T. Takenaka, K. Maruyama, and K. Sakata, "$(Bi_{1/2}Na_{1/2})TiO_3$-$BaTiO_3$ System for Lead-Free Piezoelectric Ceramics," *Jpn. J. Appl. Phys.*, **30**, 2236–9 (1991).

[9]J. Shieh, K. C. Wu, and C. S. Chen, "Switching Characteristics of MPB Compositions of $(Bi_{0.5}N_{0.5})TiO_3$-$BaTiO_3$-$(Bi_{0.5}K_{0.5})TiO_3$ Lead-Free Ferroelectric Ceramics," *Acta Mater.*, **55**, 3081–7 (2007).

[10]Z. Yu, C. Ang, R. Y. Guo, and A. S. Bhalla, "Piezoelectric and Strain Properties of $Ba(Ti_{1-X}Zr_x)O_3$ Ceramics," *J. Appl. Phys.*, **92**, 1489–93 (2002).

[11]Y. J. Dai, X. W. Zhang, and G. Y. Zhou, "Phase Transitional Behavior in $K_{0.5}N_{0.5}NbO_3$-$LiTaO_3$ Ceramics," *Appl. Phys. Lett.*, **90**, 262903 (2007).

[12]J. G. Wu, D. Q. Xiao, Y. Y. Wang, W. J. Wu, B. Zhang, and J. G. Zhu, "Improved Temperature Stability of $CaTiO_3$-Modified $[(K_{0.5}Na_{0.5})_{0.96}Li_{0.04}](Nb_{0.91}Sb_{0.05}Ta_{0.04})O_3$ Lead-Free Piezoelectric Ceramics," *J. Appl. Phys.*, **104**, 024102 (2008).

[13]J. L. Zhang, X. J. Zong, L. Wu, Y. Gao, P. Zheng, and S. F. Shao, "Polymorphic Phase Transition and Excellent Piezoelectric Performance of $(K_{0.55}Na_{0.45})_{0.965}Li_{0.035}Nb_{0.80}Ta_{0.20}O_3$ Lead-Free Ceramics," *Appl. Phys. Lett.*, **95**, 022909 (2009).

[14]E. K. Akdogan, K. Kerman, M. Abazari, and A. Safari, "Origin of High Piezoelectric Activity in Ferroelectric $(K_{0.44}Na_{0.52}Li_{0.04})(Nb_{0.84}Ta_{0.1}Sb_{0.06})O_3$ Ceramics," *Appl. Phys. Lett.*, **92**, 112908 (2008).

[15]R. P. Wang, H. Bando, T. Katsumata, Y. Inaguma, H. Taniguchi, and M. Itoh, "Tuning the Orthorhombic-Rhombohedral Phase Transition Temperature in Sodium Potassium Niobate by Incorporating Barium Zirconate," *Phys. Status Solidi RRL*, **3**, 142–4 (2009).

[16]R. Z. Zuo, J. Fu, D. Y. Lv, and Y. Liu, "Antimony Tuned Rhombohedral-Orthorhombic Phase Transition and Enhanced Piezoelectric Properties in Sodium Potassium Niobate," *J. Am. Ceram. Soc.*, **93**, 2783–7 (2010).

[17]R. Z. Zuo and J. Fu, "Rhombohedral-Tetragonal Phase Coexistence and Piezoelectric Properties of (NaK)(NbSb)O_3-$LiTaO_3$-$BaZrO_3$ Lead-Free Ceramics," *J. Am. Ceram. Soc.*, **94** [5], 1467–70 (2011).

[18]B. Jaffe, W. R. Cook, and H. Jaffe, *Piezoelectric Ceramics*. Academic Press, NY, 1971.

[19]H. L. Du, W. C. Zhou, D. M. Zhu, L. Fa, S. B. Qu, Y. Li, and Z. B. Pei, "Sintering Characteristic, Microstructure, and Dielectric Relaxor Behavior of $(K_{0.5}Na_{0.5})NbO_3$-$(Bi_{0.5}Na_{0.5})TiO_3$ Lead-Free Ceramics," *J. Am. Ceram. Soc.*, **91**, 2903–9 (2008).

[20]M. Kosec, V. Bobnar, M. Hrovat, J. Bernard, B. Malic, and J. Holc, "New Lead-Free Relaxors Based on the $K_{0.5}Na_{0.5}NbO_3$-$SrTiO_3$ Solid Solution," *J. Mater. Res.*, **19**, 1849–54 (2004).

[21]Y. P. Guo, K. Kakimoto, and H. Ohsato, "Ferroelectric-Relaxor Behavior of $(Na_{0.5}K_{0.5})NbO_3$-Based Ceramics," *J. Phys. Chem. Solids*, **65**, 1831–5 (2004).

[22]D. J. Gao, K. W. Kwok, D. M. Lin, and H. L. W. Chan, "Microstructure and Electrical Properties of La-Modified $K_{0.5}Na_{0.5}NbO_3$ Lead-Free Piezoelectric Ceramics," *J. Phys. D: Appl. Phys.*, **42**, 035411 (2009).

[23]R. Z. Zuo, C. Ye, and X. S. Fang, "Dielectric and Piezoelectric Properties of Lead Free $Na_{0.5}K_{05}NbO_3$-$BiScO_3$ Ceramics," *Jpn. J. Appl. Phys.*, **46**, 6733–6 (2007).

[24]V. Bobnar, J. Holc, M. Hrovat, and M. Kosec, "Relaxor-Like Dielectric Dynamics in the Lead-Free $K_{0.5}Na_{0.5}NbO_3$-$SrZrO_3$ Ceramic System," *J. Appl. Phys.*, **101**, 074103 (2007).

[25]C. S. Tu, C. L. Tsai, V. H. Schimidt, H. S. Luo, and Z. W. Yin, "Dielectric, Hypersonic, and Domain Anomalies of $(PbMg_{1/3}Nb_{2/3}O_3)_{1-x}(PbTiO_3)_x$ Single Crystals," *J. Appl. Phys*., **89**, 7908–16 (2001).

[26]G. C. Deng, A. Ding, G. R. Li, X. S. Zheng, W. X. Cheng, P. S. Qiu, and Q. R. Yin, "Martensitelike Spontaneous Relaxor-Normal Ferroelectric Transformation in $Pb(Zn_{1/3}Nb_{2/3})O_3$-$PbLa(Zr,Ti)O_3$ System," *J. Appl. Phys*., **98**, 094103 (2005).

[27]X. H. Zhu, J. M. Zhu, S. H. Zhou, Q. Li, Z. Y. Meng, Z. G. Liu, and N. B. Ming, "Domain Morphology Evolution Associated With the Relaxor-Normal Ferroelectric Transition in the Bi- and Zn-Modified $Pb(Ni_{1/3}Nb_{2/3}O_3$-$PbZrO_3$-$PbTiO_3$ System," *J. Eur. Ceram. Soc*., **20**, 1251–5 (2000).

[28]E. K. W. Goo, R. K. Mishra, and G. Thomas, "Electron Microscopy Study of the Ferroelectric Domains and Domain Wall Structure in $PbZr_{0.52}Ti_{0.48}O_3$," *J. Appl. Phys*., **52**, 2940–3 (1981).

[29]Z. G. Ye and M. Dong, "Morphotropic Domain Structure and Phase Transitions in Relaxor-Based Piezo-/Ferroelectric $(1-x)Pb(Mg_{1/3}Nb_{2/3})O_3$-$XPbTiO_3$ Single Crystals," *J. Appl. Phys*., **87**, 2312–9 (2000).

[30]D. I. Woodward, J. Knudsen, and I. M. Reaney, "Review of Crystal and Domain Structures in the $PbZr_xTi_{1-x}O_3$ Solid Solution," *Phys. Rev. B*, **72**, 104110 (2005).

[31]J. F. Chou, M. H. Lin, and H. Y. Lu, "Ferroelectric Domains in Pressureless-Sintered Barium Titanate," *Acta Mater*., **48**, 3569–79 (2000).

[32]G. Arlt and P. Sasko, "Domain Configuration and Equilibrium Size of Domains in $BaTiO_3$ Ceramics," *J. Appl. Phys*., **51**, 4956–60 (1980).

[33]V. Dorcet and G. Trolliard, "A Transmission Electron Microscopy Study of the A-Site Disordered Perovskite $Na_{0.5}Bi_{0.5}TiO_3$," *Acta Mater*., **56**, 1753–61 (2008).

[34]C. W. Tai and Y. Lereah, "Nanoscale Oxygen Octahedral Tilting in $0.90(Bi_{1/2}Na_{1/2})TiO_3$-$0.05(Bi_{1/2}K_{1/2})TiO_3$-$0.05BaTiO_3$ Lead-Free Perovskite Piezoelectric Ceramics," *Appl. Phys. Lett*., **95**, 062901 (2009).

[35]C. Ma, X. Tan, E. Dulkin, and M. Roth, "Domain Structure-Dielectric Property Relationship in Lead-Free $(1-x)(Bi_{1/2}N_{1/2})TiO_3$-$XBaTiO_3$ Ceramics," *J. Appl. Phys*., **108**, 104105 (2010).

[36]A. A. Bokov and Z. G. Ye, "Recent Progress in Relaxor Ferroelectrics with Perovskite Structure," *J. Mater. Sci*., **41**, 31–52 (2006).

[37]K. Uchino and S. Nomura, "Critical Exponents of the Dielectric Constants in Diffused Phase Transition Crystals," *Ferroelectr. Lett*., **44**, 55–61 (1982).

[38]D. Viehland, S. J. Jang, and L. E. Cross, "Freezing of the Polarization Fluctuations in Lead Magnesium Niobate Relaxors," *J. Appl. Phys*., **68**, 2916–21 (1990).

[39]W. Chen, X. Yao, and X. Y. Wei, "Tunability and Ferroelectric Relaxor Properties of Bismuth Strontium Titanate Ceramics," *Appl. Phys. Lett*., **90**, 182902 (2007).

[40]X. H. Dai, Z. Xu, and D. Viehland, "Normal to Relaxor Ferroelectric Transformation in Lanthanum-Modified Tetragonal-Structural Lead Zirconate Titanate Ceramics," *J. Appl. Phys*., **79**, 1021–6 (1996).

[41]V. Koval, C. Alemany, J. Briancin, H. Brunckova, and K. Saksl, "Effect of PMN Modification on Structure and Electrical Response of XPMN-(1-x) PZT Ceramic Systems," *J. Eur. Ceram. Soc*., **23**, 1157–66 (2003).

[42]X. H. Zhao, W. G Qu, H. He, N. Vittayakorn, and X. L. Tan, "Influence of Cation Order on the Electric Field-Induced Phase Transition in $Pb(Mg_{1/3}Nb_{2/3})O_3$-Based Relaxor Ferroelectrics," *J. Am. Ceram. Soc*., **89**, 202–9 (2006).

[43]J. Ricote, R. W. Whatmore, and D. J. Barber, "Studies of the Ferroelectric Domain Configuration and Polarization of Rhombohedrl PZT Ceramics," *J. Phys. Condens. Matter*, **12**, 323–37 (2000).

[44]M. S. Yoon and H. M. Jang, "Relaxor-Normal Ferroelectric Transition in Tetragonal-Rich Field of $Pb(Ni_{1/3}Nb_{2/3})O_3$-$PbTiO_3$-$PbZrO_3$ System," *J. Appl. Phys*., **77**, 3991–4001 (1995).

[45]S. M. Gupta, J. F. Li, and D. Viehland, "Coexistence of Relaxor and Normal Ferroelectric Phases in Morphotropic Phase Boundary Compositions of Lanthanum-Modified Lead Zrconate Titanate," *J. Am. Ceram. Soc*., **81**, 557–64 (1998).

[46]B. Fultz and J. M. Howe, *Transmission Electron Microscopy and Diffractometry of Materials (Third Edition)*. Springer, Berlin, Heidelberg, NY, 2007.

[47]D. Viehland, "Transmission Electron Microscopy Study of High-Zr-Content Lead Zirconate Titanate," *Phys. Rev. B*, **52**, 778–91 (1995). □